Development 129, 4613-4625 (2002)
Printed in Great Britain © The Company of Biologists Limited 2002
DEV14545

DEVELOPMENT AND DISEASE

Fgf8 is required for pharyngeal arch and cardiovascular development in the mouse

Radwan Abu-Issa[1], Graham Smyth[2], Ida Smoak[3], Ken-ichi Yamamura[4] and Erik N. Meyers[1,2,*]

[1]Department of Pediatrics, Neonatal Perinatal Research Institute, Duke University Medical Center, Durham, NC 27710, USA
[2]Department of Cell Biology, Duke University Medical Center, Durham, NC 27710, USA
[3]Department of Molecular Biomedical Sciences, North Carolina State University Raleigh, NC 27606, USA
[4]Institute of Molecular Embryology and Genetics, 4-24-1 Kuhonji, Kumamoto, 862-0976, Japan
*Author for correspondence (e-mail: meyer031@mc.duke.edu)

Accepted 1 July 2002

SUMMARY

We present here an analysis of cardiovascular and pharyngeal arch development in mouse embryos hypomorphic for *Fgf8*. Previously, we have described the generation of *Fgf8* compound heterozygous (*Fgf8*$^{neo/-}$) embryos. Although early analysis demonstrated that some of these embryos have abnormal left-right (LR) axis specification and cardiac looping reversals, the number and type of cardiac defects present at term suggested an additional role for *Fgf8* in cardiovascular development. Most *Fgf8*$^{neo/-}$ mutant embryos survive to term with abnormal cardiovascular patterning, including outflow tract, arch artery and intracardiac defects. In addition, these mutants have hypoplastic pharyngeal arches, small or absent thymus and abnormal craniofacial development. Neural crest cells (NCCs) populate the pharyngeal arches and contribute to many structures of the face, neck and cardiovascular system, suggesting that *Fgf8* may be required for NCC development. *Fgf8* is expressed within the developing pharyngeal arch ectoderm and endoderm during NCC migration through the arches. Analysis of NCC development in *Fgf8*$^{neo/-}$ mutant embryos demonstrates that NCCs are specified and migrate, but undergo cell death in areas both adjacent and distal to where *Fgf8* is normally expressed. This study defines the cardiovascular defects present in *Fgf*8 mutants and supports a role for *Fgf8* in development of all the pharyngeal arches and in NCC survival.

Key words: Fgf8, Mouse, Cardiovascular, Pharyngeal arch, DiGeorge, Neural crest, Cell death, 22q11, Double outlet right ventricle, Transposition, Arch artery, Patterning.

INTRODUCTION

Fgf8, a member of the extracellular signaling fibroblast growth factor (Fgf) family, is required for a variety of patterning events during vertebrate development. In chick and zebrafish, several studies have implicated *Fgf8* in craniofacial (Farrell et al., 2001; Schneider et al., 2001) and cardiovascular development (Alsan and Schultheiss, 2002; Reifers et al., 2000). In mouse, *Fgf8* is required early in development as *Fgf8* homozygous null embryos arrest at gastrulation with a failure of mesoderm to migrate out of the primitive streak (Sun et al., 1999). Tissue-specific deletions using Cre recombinase strategies have confirmed roles for *Fgf8* in later developmental events as well. Deletion of *Fgf8* in the apical ectodermal ridge of the developing limb bud results in limb defects (Lewandoski et al., 2000; Moon and Capecchi, 2000), while deletion of *Fgf8* within the first pharyngeal arch (PA) results in loss of structures derived from the first arch due to NCC death (Trumpp et al., 1999).

Previously, we have targeted the *Fgf8* gene locus to generate an allelic series of mutations. In addition to a null allele (*Fgf8*$^{tm1.4Mrt}$ or *Fgf8*$^{-}$) and a Cre recombinase-dependent floxed allele of *Fgf8* (*Fgf8*$^{tm1.3Mrt}$ or *Fgf8*^{Flox}), we have generated a hypomorphic allele (*Fgf8*$^{tm1.1Mrt}$ or *Fgf8*^{neo}) that variably lowers the level of functional *Fgf8* mRNA (Meyers et al., 1998). The development of compound heterozygous (*Fgf8*$^{neo/-}$) embryos (herein termed *Fgf8* mutants) is variable, with ~20% resembling the *Fgf8*$^{-/-}$ gastrulation phenotype or less severe gastrulation defects. These embryos arrest development between embryonic day (E) 7.5 and E9.5. The remaining 80% of *Fgf8*$^{neo/-}$ embryos progress to term with neural, limb, craniofacial and/or cardiac defects.

Previously, we have also shown that some of these embryos have abnormalities in left-right axis (LR) determination with cardiac looping abnormalities. Cardiac looping was reversed in 21% and failure or midline looping occurred in 28% (~20% in the current study), while ~50% had pulmonary isomerism or abnormal *Nodal* expression (Meyers and Martin, 1999). The embryos with midline/failure of looping arrest development at E9.5. This suggests therefore, that at near term, the number of

surviving embryos with atrioventricular discordance (looping reversal) in this study should be ~30%. This study focuses on the PA and cardiovascular development of the *Fgf8*$^{neo/-}$ embryos that survive early defects, ~50% of which potentially have abnormal LR axis specification.

NCCs are ecto-mesenchymal cells that migrate from the extreme dorsal surface of the embryo to populate numerous structures along the dorsoventral axis. Cranial neural crest arises from the forebrain and hindbrain region to populate craniofacial structures as well as PA1-3, giving rise to the maxilla, mandible as well as other structures of the neck and face. Cardiac neural crest has been defined in the chick as originating between the otic placode and the third somite (Kuratani and Kirby, 1992; Nishibatake et al., 1987). These cells populate the third, fourth and sixth PAs, as well as the outflow tract of the heart. Many of the original NCC fate map studies in chick have more recently been confirmed in the mouse through use of the Cre/*LoxP* transgenic system to lineage trace neural crest derivatives (Jiang et al., 2000; Li et al., 2000; Yamauchi et al., 1999).

NCCs are essential for cardiovascular patterning and experimental models that ablate cardiac NCCs result in characteristic cardiovascular abnormalities such as failure of outflow tract septation and aortic arch artery defects (reviewed by Kirby and Waldo, 1995). In addition, several mouse genetic models with abnormal NCC development also have these characteristic cardiovascular abnormalities (reviewed by Maschhoff and Baldwin, 2000). Several human birth defect syndromes, collectively termed 22q11 deletion syndromes, are thought to result from defects in NCC development. Cardiovascular defects include no outflow tract septation (persistent truncus arteriosus), abnormal septation (double outlet right ventricle, tetralogy of Fallot), or abnormal patterning of the aortic arch arteries leading to interruption of the aortic arch and aberrant vascular structures. Craniofacial findings in these syndromes can include cleft palate, abnormal facial features as well as external ear defects. Deficiencies of other NCC-dependent structures such as the thymus and parathyroids are seen as well (reviewed by Lindsay, 2001).

In this study we present an analysis of the cardiovascular and PA phenotypes present in *Fgf8*$^{neo/-}$ embryos. *Fgf8* mutants have defects in many NCC-derived cardiovascular and craniofacial structures that mimic the 22q11 deletion syndromes. These novel phenotypes define a role for *Fgf8* in cardiovascular, PA and NCC development.

MATERIALS AND METHODS

Generation of *Fgf8*$^{neo/-}$ embryos

For efficiency, *Fgf8*$^{neo/-}$ embryos were generated taking advantage of the Cre/*LoxP* system. Previously, mice that contain *Fgf8* sequences flanked by loxP (Floxed) sequences have been used for the generation of *Fgf8*$^{Flox/-}$ embryos also transgenic for the *Msx2-Cre* gene (Lewandoski et al., 2000). These mice are viable with only limb defects as *Msx2-Cre* expression is restricted to the apical ectodermal ridge of the developing limb bud. However, because the *Msx2-Cre* transgene is also active in the adult male germline, males of the genotype *Fgf8*$^{Flox/-}$::*Msx2-Cre* only pass the *Fgf8* null allele to offspring because the remaining *Fgf8*^{Flox} allele is recombined prior to fertilization. We therefore crossed *Fgf8*$^{Flox/-}$::*Msx2-Cre* males to *Fgf8*$^{neo/+}$ females to generate litters in which 50% of the embryos were *Fgf8*$^{neo/-}$. Although half of these embryos remain transgenic for *Msx2-Cre*, the presence of this transgene had no bearing on the phenotype analyzed in this study, as *Fgf8*$^{neo/-}$ and *Fgf8*$^{neo/-}$::*Msx2-Cre* embryos had similar phenotypes except for limb defects. Embryonic day 0.5 was defined as noon the day a vaginal plug was noted. Embryos were maintained on an outbred ICR background to increase fecundity as we observed no gross differences in the phenotype of *Fgf8*$^{neo/-}$ embryos at term when compared to an inbred 129 background. This outbred background did however lower the percentage of embryos that were lost to earlier gastrulation defects from 28% to roughly 20% (Meyers and Martin, 1999).

Generation of *Fgf8*$^{neo/-}$:: *Tie2-lacZ* embryos

To follow endothelial cell development, we established *Fgf8*$^{+/-}$ mice that were transgenic for the *Tie2-lacZ* transgene in which *lacZ* is controlled by a *Tie2* endothelial cell promoter element (Schlaeger et al., 1997). *Fgf8*$^{+/-}$::*Tie2-lacZ* males were then crossed to *Fgf8*$^{neo/+}$ females to generate control and *Fgf8*$^{neo/-}$ embryos also transgenic for *Tie2-lacZ*. Embryos were examined for β-Galactosidase (β-Gal) activity and cleared in a 50% glycerol/phosphate buffered saline (PBS) solution for visualization. Of note, the pericardial sac was removed prior to staining and the embryos were rotated slowly at 37°C to improve penetration of deep tissue.

Generation of *Fgf8*$^{neo/-}$::*R26R*::*P0-Cre* embryos

To lineage trace NCCS in *Fgf8* mutants, we generated males that were *Fgf8*$^{+/-}$ and transgenic for *P0-Cre* (Yamauchi et al., 1999), and crossed these to *Fgf8*$^{neo/+}$ females also transgenic for the Cre reporter transgenic line *R26R* (Soriano, 1999). Embryos were then fixed and stained for β-Gal activity. Embryos were cleared as above.

In situ hybridization

Whole-mount mRNA in situ hybridization was performed essentially as described (Neubuser et al., 1997) using digoxigenin antisense riboprobes constructed from linearized plasmids. All in situ results were confirmed in at least three mutant and three control embryos treated identically.

Immunohistochemistry

Immunohistochemistry was performed on embryos fixed in 4% PFA (overnight 4°C) and washed in PBT (PBS with 0.1%Triton X-100). Embryos were blocked (PBT, 3% BSA, 10% sheep serum) for 1 hour followed by incubation (in block) with/without primary antibody at 4°C overnight. Embryos were then washed in 1:5 block:PBT three times for 1 hour each. Embryos were incubated overnight with secondary antibody in block followed by washing (3×1 hour each) in 1:5 block:PBT and then mounted with DABCO.

Whole-mount cranial nerves were visualized with monoclonal 2H3 antibody (Developmental Studies Hybridoma Bank and developed by T. Jessel and J. Dodd) as described (Swiatek and Gridley, 1993). Embryos were washed and alkaline phosphatase-conjugated secondary antibody added. Embryos were washed again and then stained for alkaline phosphatase with NBT/BCIP in 0.1 mM levamisole.

Whole-mount proliferation was performed by detecting cells in metaphase with anti-phosphorylated histone H3 IgG (Upstate Biotechnology) and an Alexa Red secondary antibody (Molecular Probes). Embryos were then dehydrated, cleared and mounted for confocal analysis as described (Zucker et al., 1999).

Cell death

Whole-mount cell death was performed using Lysotracker Red (Molecular Probes) essentially as described (Zucker et al., 1999) with the following modifications: sterile lactated ringers was substituted for Tyrode's buffer; 2-4 μM Lysotracker was used for 30 minutes while rotating at 37°C in an air filled tube; embryos were washed three times in lactated ringers and then four times in PBS over the course of 30

minutes at room temperature with gentle inversion; embryos were then fixed, dehydrated and cleared as described.

TUNEL assay (Roche) was performed on *PO-Cre::R26R*::*Fgf8*$^{neo/-}$ embryos that were first stained for *lacZ* in whole mount. Embryos were dehydrated, embedded in paraffin wax and sectioned at 6 μm. TUNEL was then performed essentially as described by the manufacturer.

Genotyping

Fgf8$^{neo/-}$ embryos are identifiable as early as E8.5 by defects at the mid-hindbrain boundary. Heterozygous adult mice and embryos at earlier stages were genotyped as described (Meyers and Martin, 1999). *P0-Cre* and *Msx2-Cre* transgenic mice were genotyped using the PCR primers (5′ TGATGAGGTTCGCAAGAACC:: 3′ CCATGAGTGAACGAACCTGG) contained within the Cre gene; *R26R* and *Tie2-lacZ* transgenic mice were genotyped using the PCR primers (5′ ATCCTCTGCATGGTCAGGTC:: 3′ CGTGGCCTGATTCATTCC) contained within the *lacZ* gene. Throughout the study, *Fgf8*$^{+/+}$, *Fgf8*$^{neo/+}$ or *Fgf8*$^{+/-}$ littermate embryos were considered wild-type/control embryos as they demonstrate no identifiable phenotype.

Confocal analysis

Embryos where indicated were analyzed on a Zeiss LSM 410 laser-scanning confocal microscope. For cell death and proliferation, *z*-sectioning series were done with single pass 1-4 μm sections. Sections were then stacked and converted to Quicktime movie images using NIH Image v. 1.62 software for serial viewing.

Ectopic application of FGF8

ICR mouse E9.5 embryos were incubated in stationary culture (DMEM with 20% fetal calf serum, penicillin and streptomycin antibiotics). Heparin beads (Sigma H5263) were coated with 1 mg/ml FGF8 protein (b isoform; R&D Systems) or PBS with 1 mg/ml BSA. Embryos were placed on their left sides and 1-3 beads were placed over the right caudal arches. Embryos were then cultured for 4-6 hours at 37° and 5% CO_2. Media was washed off and embryos fixed overnight in 4% paraformaldehyde in preparation for in situ hybridization.

RESULTS

Fgf8$^{neo/-}$ embryos survive to term with complex cardiac defects.

We examined *Fgf8*$^{neo/-}$ embryos from E16.5 to term for cardiac patterning defects. Gross abnormalities in heart development were present in 66% (79/119) of mutant embryos but less than 1% of control littermates. The most common defects were outflow tract anomalies, consisting primarily of malpositioned or transposed aortic and pulmonary arteries. The aorta normally arises from the left ventricle posterior and left of the pulmonary artery (Fig. 1A,D). However, in 56% (67/119) of mutant embryos the aorta arose from the right ventricle, either ventral or adjacent to the pulmonary artery of mutants. In addition, most of these transposed mutants (83%) displayed double outlet right ventricle as both arteries appeared to arise from the right ventricle, often with a hypoplastic pulmonary artery (Fig. 1B and data not shown). External diagnosis of double outlet right ventricle was confirmed in seven out of eight mutant embryos examined by sectioning (Fig. 1E and data not shown). Eight percent (10/119) of mutants had complete failure of outflow tract septation or persistent truncus arteriosus with the branch pulmonary arteries arising from the ascending single outflow

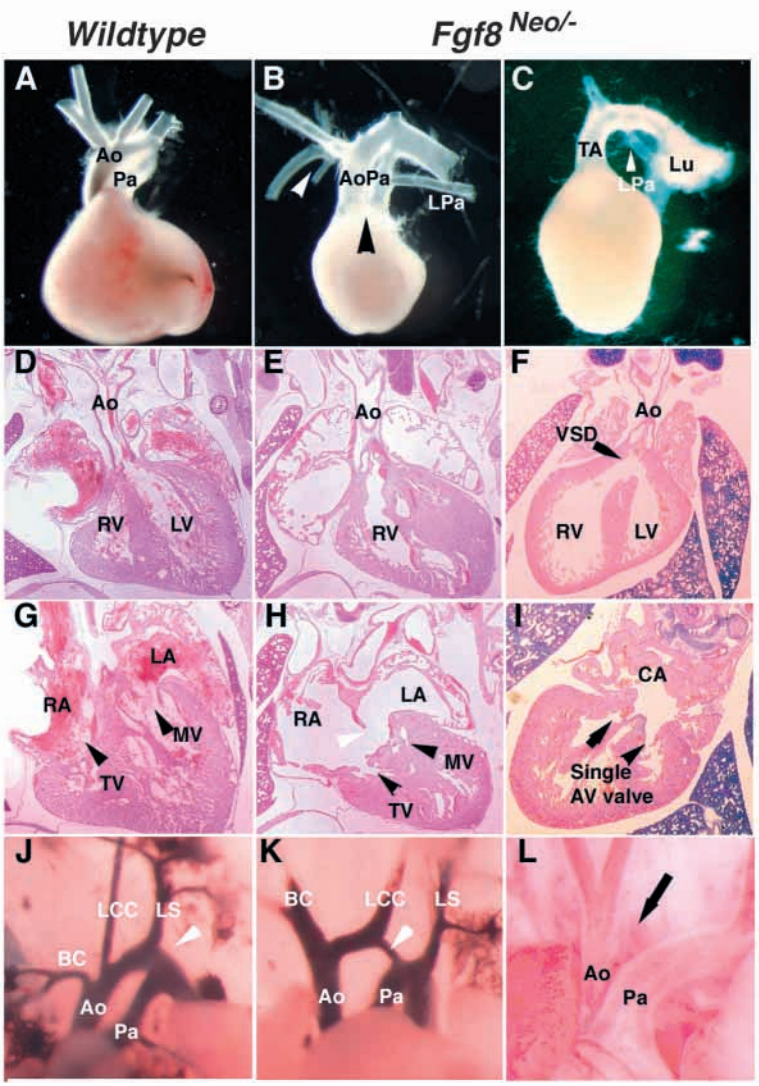

Fig. 1. (A) Normal anatomy with the aorta (Ao) arising to the left and dorsal to the pulmonary artery (Pa). (B) *Fgf8* mutants had frequent transposition with the Ao arising to the right and adjacent to the Pa (black arrowhead), and also an abnormal subclavian artery pattern (white arrowhead). (C) Less frequently there was persistent truncus arteriosus (TA). Note left branch pulmonary artery (LPa) arising from Ao to supply lung (Lu) (white arrowhead in C). In wild type (D), the Ao arises from the left ventricle (LV), while in *Fgf8* mutant (E) the Ao arises from the right ventricle (RV). In another mutant (F), a single outflow tract arising from both the RV and LV over-rides a ventricular septal defect (VSD). *Fgf8* mutants had atrial septal defects (white arrowhead H) or common atrium (CA) (I). In addition, although normally the right and left ventricles are separated from the right atrium (RA) and left atrium (LA) by the tricuspid (TV) and mitral valves (MV), respectively (G,H), several mutants had a single atrioventricular valve (I, black arrowheads). In addition to these abnormalities, ink injections/inspection of near-term embryos demonstrated a normal sized aortic arch in wild type (white arrowhead in J) although *Fgf8* mutants often had hypoplastic (white arrowhead in K) or completely absent (black arrow in L) aortic arch, which is derived from the fourth arch artery. BC, braciocephalic; LCC, left common carotid; LS, left subclavian.

Table 1. Summary of *Fgf8* mutant cardiovascular phenotypes

	Outflow tract defects			
	Transposition	Persistent truncus arteriosus	Grossly normal outflow tract	Number of mutants examined
	67 (56%)*	10 (8%)	40 (34%)	119†

	Aortic arch artery defects			
	Hypoplastic or IAA	Abnormal subclavian artery/reversed arch	Normal arch artery pattern	Number of mutants examined
E16.5-E18.5	16 (13%)	36 (30%)	67 (57%)	119
E9.5-E10.5	18 (79%)‡		5 (21%)	23

	Intracardiac defects§			
	ASD	VSD	AV-valve	
	12 (100%)	12 (100%)	2 (16%)¶	12

*The majority (56/67 or 83%) of mutant embryos with transposition appeared to have double outlet right ventricle with both the transposed aorta and pulmonary artery arising from the right ventricle. In the remaining embryos with transposition, the origin of the pulmonary artery was not clear secondary to hypoplasia of the artery. Histological sections confirmed this external observation in seven out of eight mutant embryos that appeared to have double outlet right ventricle.

†Two (2%) mutant embryos had situs inversus totalis to complete the 119 embryos.

‡Embryos examined at E9.5-E10.5 had third and/or fourth arch artery defects. Presumably the number of mutants that appear normal is greater near term due to recovery of earlier apparent defects (see text).

§Only mutant embryos that appeared to have abnormal external structures were sectioned and examined.

¶Both of these embryos had an abnormally shaped heart with the cardiac apex pointing to the right, suggesting an earlier cardiac looping reversal.

IAA, interrupted aortic arch; ASD, atrial septal defect; VSD, ventricular septal defect; AV, atrioventricular.

tract (Fig. 1C,F). Two percent (2/119) embryos had situs inversus with mirror image reversal of the heart and outflow tract vessels (data not shown). These data are summarized in Table 1.

In addition to and independent of the above outflow tract abnormalities, hypoplastic or complete interruption of the aortic arch (Fig. 1 compare J to K,L) was present in 13% (16/119) of embryos. Aortic arch artery patterning was abnormal with aberrant origins of the subclavian and carotid arteries (Fig. 1B, white arrowhead) as well as a right sided aortic arch and descending aorta in 30% of mutant embryos (data not shown).

In addition to these extracardiac defects, there were intracardiac defects as well in *Fgf8*$^{neo/-}$ embryos. The left ventricle was often hypoplastic (compare Fig. 1A with 1B) and histological analysis revealed atrial and ventricular septal defects in all mutants examined (n=12) that had outflow tract defects (Fig. 1H,I). In addition, two of the 12 sectioned mutants had defects in the atrioventricular junction consisting of a singular atrioventricular valve (Fig. 1I). Thirty-four percent (40/119) of mutants had grossly normal cardiac development, most likely reflecting the variable reduction in *Fgf8* expression characteristic of the hypomorphic allele (Meyers et al., 1998).

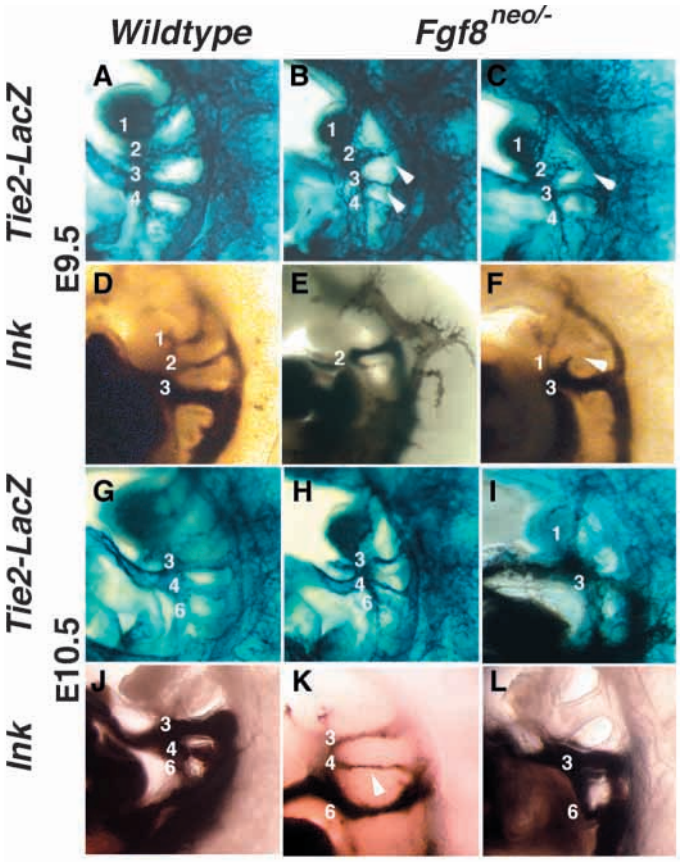

Fig. 2. Left side views of whole-mount transgenic Tie2-*lacZ* (A-C,G-I) (see Materials and Methods) and ink injections (D-F,J-L) demonstrate abnormal arch artery patterning in *Fgf8* mutant embryos. At E9.5, (A-F) endothelial cells of the first through third arch arteries are normally well developed in wild type embryos (A), while in *Fgf8* mutants the arch arteries were often hypoplastic (arrowheads in B). In addition, the second arch was often proximally interrupted (arrowhead, C). These findings were essentially confirmed by ink injection (compare D with E,F). At E10.5 (G-L), the third, fourth and sixth arch arteries are well formed in wild type (G), while in *Fgf8* mutants they were often hypoplastic (H) or completely missing, as the second and fourth are in I (note embryo in I was also ink injected). Similarly, ink injections demonstrate hypoplastic (arrowhead in K) or absent (L) fourth arch artery in *Fgf8* mutants when compared with control (J).

Fgf8$^{neo/-}$ embryos have defective aortic arch artery development

In order to understand how these cardiovascular defects arose from loss of *Fgf8*, we examined cardiovascular development between E8.5 and E10.5 using the endothelial cell marking *Tie2-lacZ* transgene (Schlaeger et al., 1997) to visualize arch artery development in *Fgf8* mutants (n=23) and controls (n=37). Seventy-eight percent (18/23) of *Fgf8*$^{neo/-}$ mutant embryos had gross defects in the endothelial pattern of the arch arteries. In E9.5 wild-type embryos, arch arteries 1-3 are well formed while the fourth is beginning to form (Fig. 2A). These arteries were often smaller or absent in similar stage mutants (Fig. 2B,C). At E10.5 the third, fourth and sixth arch arteries of wild type are readily apparent (Fig. 2G), while defects, including hypoplasia or complete absence of the third and/or fourth arch arteries, was

present in 60% (14/23) of *Fgf8* mutants (Fig. 2H,I). We did not detect a LR bias to the defects seen in *Fgf8* mutants as nine had bilateral, five had left-sided and four had right-sided defects.

In addition to the endothelial defects present, we also tested patency of the arch arteries in *Fgf8* mutants by injecting India ink into the right ventricle of several mutants and controls. The result of these injections essentially confirmed the findings of the *Tie2-lacZ* transgenic *Fgf8* mutant embryos. At E9.5, *Fgf8* mutants often lacked one or more of the three patent arteries seen in wild-type embryos (compare Fig. 2D with 2E and 2F). At E10.5, the third and/or fourth arch arteries were hypoplastic (Fig. 2K) or completely missing (Fig. 2L) in the majority of mutants. These findings are consistent with the arch artery patterning defects noted at term in *Fgf8* mutant embryos. Interestingly, the percentage of mutant embryos with arch artery defects at E10.5 was higher than that observed near term, suggesting that some embryos recover from earlier defects or that some vascular structures substitute for missing structures as proposed previously (Lindsay and Baldini, 2001; Waldo et al., 1996).

Fgf8$^{neo/-}$ embryos have abnormal pharyngeal arch development

One of the most striking defects on gross examination of *Fgf8*$^{neo/-}$ embryos at earlier stages is abnormal development of the PAs. As early as E8.0, hypoplasia of the first PA can be identified; by E10.5, *Fgf8* mutants have obviously smaller first and second pharyngeal arches (compare Fig. 3A with 3B). These arches show a reduction in both total size, but also in the formation of the pharyngeal clefts, which are the ectodermal junctions between arches (compare Fig. 3C with 3D and arrowheads in 3E with those in 3F). Besides the clefts, the PAs also have internal endodermal pouches that delineate each arch. The first two endothelial pouches appeared grossly intact (Fig. 3C,D). More caudal, the third and fourth arches were small or absent in *Fgf8* mutants as well, when examined by laser confocal optical section (Fig. 3E,F). Pharyngeal pouches 3 and 4 were difficult to identify in mutants, suggesting they were also small or absent. To better define the pouches, we examined the expression of *Pax1*, which is expressed in the developing endodermal pouches (Deutsch et al., 1988). While *Pax1* was expressed in the first and second pouch (Fig. 3G,H), the expression was abnormal with a fusion of these two pouches. This is consistent with the absence of the more proximal region of the second PA we have observed in some of these embryos (Fig. 2C, arrowhead). In addition, later stages demonstrated loss of *Pax1* expression in the caudal pouches of mutants (Fig. 3I,J), presumably because these structures were absent, consistent with the morphological examination.

Structures derived from the arches are deficient in *Fgf8*$^{neo/-}$ embryos

The majority of pharyngeal arch tissue is derived from migratory NCCs, with other contributions from endoderm, ectoderm and paraxial/lateral plate mesoderm. NCCs are not only required for development of the arch arteries and outflow tract septation, but also for development of several other structures, including craniofacial bones, endocrine organs of the neck, otic ossicles, sympathetic ganglia and cranial nerve ganglia. The cardiovascular defects described above are consistent with abnormal NCC development. To assay for defects of other NCC-derived structures, we first examined bone preparations of *Fgf8*$^{neo/-}$ embryos. It should be noted that virtually all *Fgf8* mutants examined had the craniofacial defects described unless otherwise stated.

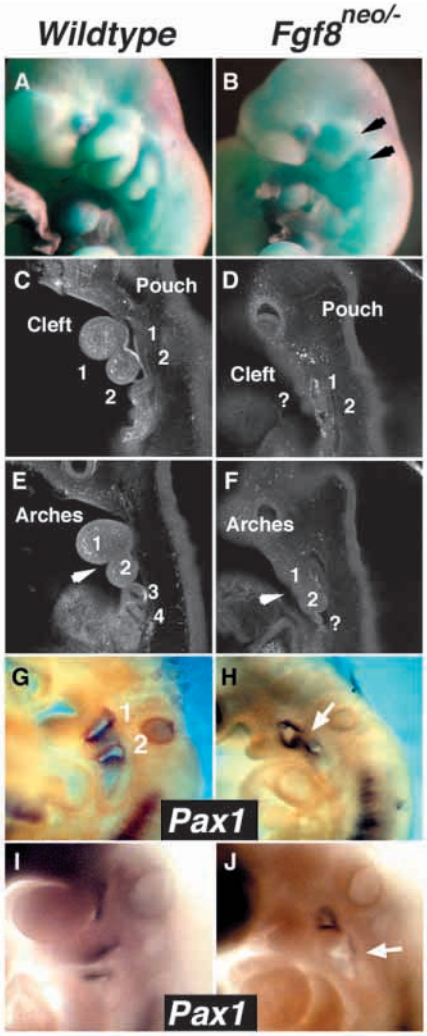

Fig. 3. Gross morphology of E10.5 embryos demonstrate the first and second arch to be much smaller and fused in *Fgf8* mutants (arrows in B, compare with A). Confocal optical sectioning through the arches revealed the absence of pharyngeal clefts 1 and 2 (compare D with C and arrowhead in E with F), while the upper pharyngeal pouches were roughly intact (compare pouches 1 and 2 in D and C). The caudal pharyngeal arches were often absent as well (compare 3 and 4 in E with F). *Pax1*, which is expressed in the pharyngeal pouch endoderm at E9.5 (G,H) and E10.5 (I,J), is abnormal in *Fgf8* mutants (H,J) when compared with controls. Note gap in arch 2 (arrow, H) and loss of expression (arrow, J).

The first PA develops as two distinct rostral and caudal structures, termed the maxillary and the mandibular components, respectively. The maxillary component contributes to the maxilla, zygomatic arch, squamosal bone and a region of the palate. Defects in all of these structures are seen in *Fgf8*$^{neo/-}$ embryos (Fig. 4A,B and data not shown). The mandibular component contributes to Meckel's cartilage, which forms the malleus and incus (middle ear bones) and supports mandible

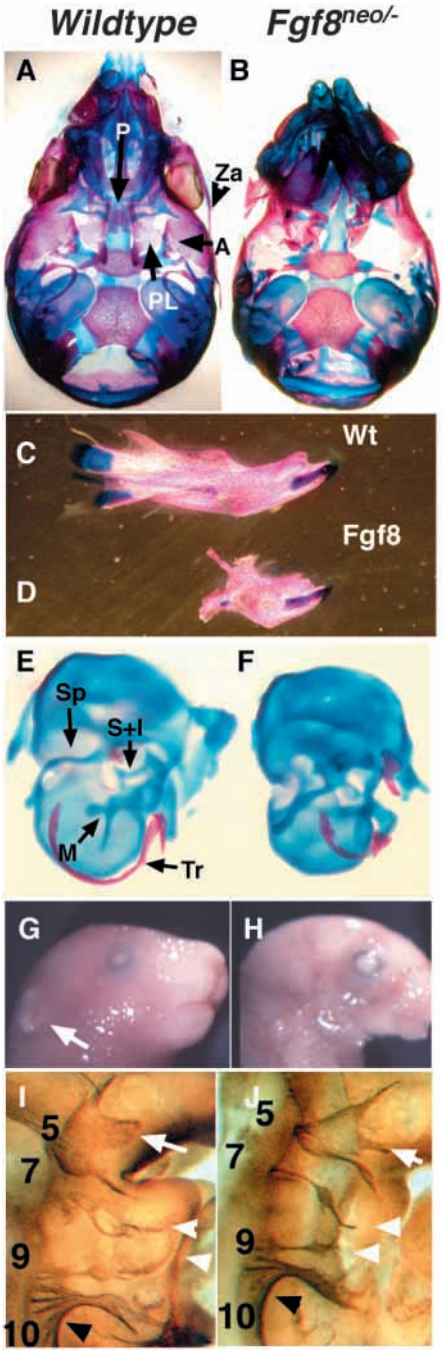

Fig. 4. E18.5 skull bone preparations (A-F) of wild-type (A,C,E,G,I) and *Fgf8* mutants (B,D,F,H,J) demonstrate abnormal development of the palate (P), palatine (PL), alisphenoid (A) and zygomatic arch (Za). The mandibles of *Fgf8* mutants were extremely hypoplastic, sparing only the most distal structures (compare C with D). Defects in the styloid process (Sp), tympanic rings (Tr), stapes, incus (S+I), and malleus (M) are observed as well in mutants (F) when compared with wild type (E). *Fgf8* mutants also had abnormal or absent external ears (compare arrow in G with H). Immunohistochemistry for the 2H3 antibody demonstrated that cranial nerves 5, 7, 9 and 10 were fairly well formed in wild type (I), with reduction in *Fgf8* mutants (J) of the distal tips (compare arrowheads in I to J), and narrowing of the facial branch of cranial nerve 5 (arrow, J). In addition, nerve 10 had fewer ramifications proximally (compare black arrowhead in I with that in J).

development. Again, defects in all three of these structures occurred with absent or severely hypoplastic Meckel's cartilage (data not shown), absent malleus and incus, as well as a severely defective mandible and tympanic ring (Fig. 4C-F). Other craniofacial defects included reduced or absent alisphenoid, presphenoid, squamosal, pterygoid, palatine and alatemporalis bones (Fig. 3A,B and data not shown).

NCCs contribute to tooth development as well. Previously, *Fgf8* had been implicated in tooth induction in the chick (Neubuser et al., 1997). *Fgf8*$^{neo/-}$ embryos lacked the molar region and therefore molar teeth; however, distal incisors were intact despite severe jaw defects (Fig. 4D). This suggests that distal but not proximal elements of the first PA require *Fgf8* and is consistent with a first PA-specific ablation of *Fgf8* (Trumpp et al., 1999). Alternatively, in both the tissue specific ablation study and in our study, residual *Fgf8* function may result in the formation of the incisor.

The second PA gives rise to Reichert's cartilage, which in turn contributes to the stapes, as well as the styloid process and the dorsal aspect of the hyoid bone. In *Fgf8*$^{neo/-}$ embryos, the stapes was normal or slightly smaller while the styloid process was thickened and/or shortened (Fig. 4E,F). Although most were normal, a small number of *Fgf8* mutants had mild defects in the hyoid bone. The mild nature of this defect is surprising given the severe defects noted in arch 2 earlier in development (Fig. 2C, Fig. 3B,H). The external ear, which develops from several hillocks at the dorsal base of the first and second arch, was also either hypoplastic or completely absent in a majority of *Fgf8* mutants, suggesting proximal segments of the first two arches are defective as well (Fig. 4G,H).

The third and fourth arches contribute to laryngeal cartilages as well as to several glands in the neck including the thymus, thyroid and parathyroid glands. The thymus of most mutants were smaller, single lobed or completely absent (data not shown). In addition, some mutant embryos had a reduction in the size and number of sub-mandibular glands. Minor defects in the laryngeal cartilages of *Fgf8* mutants occurred but were rare.

We next examined the development of the NCC-derived cranial nerves. We found subtle defects in the development of cranial nerves 4, 5, 7, 9 and 10. The trochlear (4) was completely absent (data not shown), most probably as a result of the deletion of the mid-hindbrain (from which the fourth nerve arises) previously described in these mutants (Meyers et al., 1998). Cranial nerves 5, 7, 9 and 10 had truncated end processes consistent with the loss of arch and craniofacial tissue described above (Fig. 4I,J). The grossly normal size and location of the nerves suggested that these abnormalities are secondary to loss of target tissues and not due to abnormal specification or patterning of the cranial nerves themselves.

Neural crest is specified and migrates in *Fgf8*$^{neo/-}$ embryos

Most or all of the above defects are consistent with abnormal development of the PAs and more specifically of the cranial and cardiac NCCs. Given the defects we observed in NCC-derived structures, we next sought to determine if NCCs are specified and migrate in *Fgf8* mutant embryos. We examined

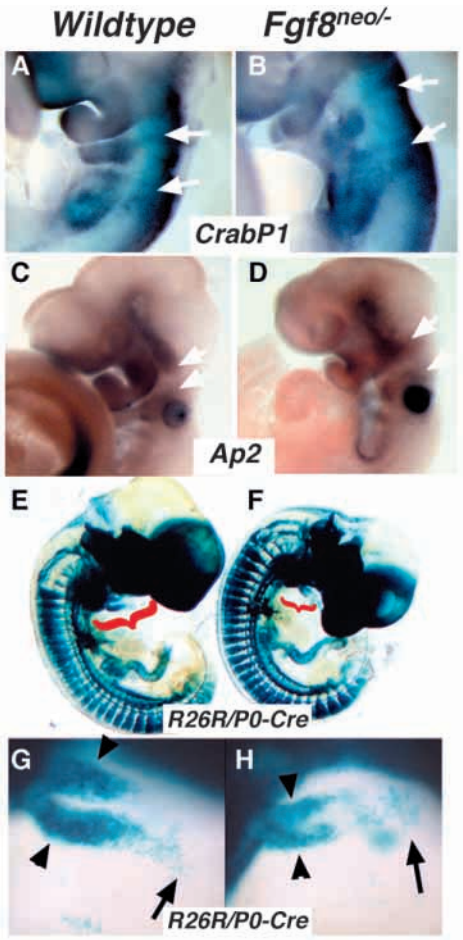

Fig. 5. mRNA in situ hybridization for two neural crest markers CrabP1 and Ap2α revealed a similar NCCs stream between wild type and *Fgf8* mutants for second and third PA (arrows in A,B) and first and second PA (arrows in C,D). Lineage trace of NCCs using the transgenic lines *P0-Cre* and *R26R* (E,F) (see Materials and Methods) demonstrated decreased NCCs within the PAs. High-powered examination of the outflow tract (red brackets in E,F) also demonstrated that decreased NCCs were entering the outflow tract of *Fgf8* mutants (arrowheads, H) when compared with controls (arrowheads, G), despite NCCs having progressed as far into the outflow tract (arrows in G,H). G and H are at the same magnification and embryos had the same number of somites (±2).

two markers, *Crabp1* and *Ap2a*, both expressed in migrating NCCs (Dencker et al., 1990; Mitchell et al., 1991). *Ap2a* (Fig. 5A,B) and *Crabp1* (Fig. 5C,D) were grossly normal in quantity and migration pattern when examined in *Fgf8* mutants at E9.5. However, at later stages (E10.5), a mild reduction was seen in the expression of both markers, suggesting that NCCs are specified and migrate but are not maintained (data not shown).

Fgf8$^{neo/-}$ embryos have a reduced amount of NCCs

In order to study the fate of NCCs in more detail, we performed a genetic lineage trace of NCCs in *Fgf8*$^{neo/-}$ embryos using a *Cre* transgene expressed in migrating NCCs (*P0-Cre*) and the *Cre* reporter line termed *R26R*. This reporter gene irreversibly expresses *lacZ* once cells have undergone CRE recombination (Soriano, 1999). By crossing the *P0-Cre* and R26R transgene, onto the *Fgf8*$^{neo/-}$ background and *R26R* onto the *Fgf8*$^{neo/-}$ background, we generated *Fgf8*$^{neo/-}$ and wild-type embryos that contained lineage-marked NCCs. It should be noted that *Fgf8* is not expressed in NCCs, thus the consequence of recombining the *Fgf8*^{neo} allele by *P0-Cre* has no gross effect on cardiovascular development in these embryos (E. N. M., unpublished).

At E10.5, there was a modest decrease in the domain that was β-Gal-positive in the pharyngeal arches, suggesting that loss of arch tissue at least partially results from loss of NCCs (Fig. 5E,F, red brackets). In addition, we also noted decreased NCCs entering the outflow tract of the heart. Normally, the NCCs enter the outflow tract of the heart in two discrete prongs (Fig. 5G). When *Fgf8* mutants (n=5) were compared with controls (n=15) stage matched for somite number (±2 somites), the prongs of NCCs were either smaller (Fig. 5H) or almost completely absent (data not shown; n=1). These prongs were smaller, despite NCCs traveling a similar distance into the outflow tract when compared with controls, confirming that they were at a comparable stage of development (arrows Fig. 5H). It should also be noted that all stage-matched controls displayed similar prongs in the outflow tract, suggesting that *PO-Cre* was giving a consistent recombination pattern and that the timing of NCCs entering the outflow tract was also relatively consistent between wild-type embryos at the same somite stage.

NCCs proliferate normally in *Fgf8*$^{neo/-}$ embryos

A reduction of NCCs in *Fgf8*$^{neo/-}$ embryos after specification and migration indicates either an abnormality in proliferation or survival of NCCs in the absence of normal levels of *Fgf8*. We first examined proliferation using an antiphospho-histone H3 antibody to mark cells in metaphase. Whole-mount embryos were then examined using confocal laser microscopy optical sections (see Materials and Methods). Representative confocal sections of E9.5 embryos are shown in Fig. 6A-C. We were unable to detect a significant difference of proliferation within the arches of *Fgf8*$^{neo/-}$ embryos (n=3) when compared with control littermates. However, we cannot rule out that subtle differences in proliferation, or changes in proliferation occurring at earlier stages, are contributing to the decreased NCCs seen in these mutants.

Fgf8$^{neo/-}$ embryos show increased cell death in areas of NCC migration

We next examined cell survival in whole-mount *Fgf8*$^{neo/-}$ embryos by using a fluorophore (Lysotracker Red, Molecular Probes) that fluoresces in necrotic and/or apoptotic cells (Zucker et al., 1999). Strikingly, there were marked areas of increased cell death in *Fgf8*$^{neo/-}$ embryos. At E8.0, there was a small amount of cell death in wild-type embryos in the area of the anterior neural ridge and mid-hindbrain region (Fig. 6D). In *Fgf8*$^{neo/-}$ embryos there was increased apoptosis in the anterior neural ridge of the developing nervous system (Fig. 6E, arrow), near the developing inflow tract of the heart, and along the flank adjacent to this area (Fig. 6E, arrowhead). Some *Fgf8*$^{neo/-}$ embryos had a marked increase of death in cells leaving the neural tube (Fig. 6E asterisks, compare with 6D), as well as in cells within the developing somites (data not shown). At E8.5, there continued to be small amounts of cell death in the forebrain and at the mid-hindbrain boundary of controls (Fig. 6G). *Fgf8* mutants had a marked increase in cell

death in the developing forebrain and mid-hindbrain junction (Fig. 6H, arrows), consistent with the holoprosencephaly and mid-hindbrain deletions present in these mutants (Meyers et al., 1998). At E9.5, there were several small areas of cell death in wild-type embryos: first, a moderate population migrating from the mid-hindbrain region into the first PA (data not shown); second, a smaller population immediately around the developing otocyst; and finally, a population at the proximal junction of the first and second arch (Fig. 6J,M). In *Fgf8*$^{neo/-}$ embryos, there was a dramatic increase in cell death in cells of the developing arches, as well as continued cell death near the mid-hindbrain junction (Fig. 6K). More lateral optical sections revealed that a large population of presumptive NCCs between the mid-hindbrain boundary and the first arch as well as cells entering the second and third arch were dying in *Fgf8* mutants but not in controls (Fig. 6M,N). At E10.5, increased cell death continued in the arches of *Fgf8* mutants, however, it appeared more restricted to the endodermal clefts and pouches (data not shown).

Fgf8 expression correlates with areas of cell death

We performed whole-mount *Fgf8* mRNA in situ hybridization to determine the expression pattern of *Fgf8* in wild-type embryos relative to the areas of cell death seen in *Fgf8* mutants. Strikingly, the expression of *Fgf8* in the developing arches corresponds well with the areas of increased cell death seen in the mutants. At E8.0, *Fgf8* expression in the forebrain and lower arches closely approximates the apoptosis seen (compare arrow and arrowheads in Fig. 6E,F). At E8.5, there continues to be increased death either adjacent to or immediately below the arch expression of *Fgf8*, while new cell death is occurring in the mid-hindbrain region where *Fgf8* is also expressed (compare Fig. 6H with 6I). At E9.5, the area of cell death caudal to the otocyst appears adjacent or immediately dorsal to a broad domain of *Fgf8* mRNA expression (compare Fig. 6K with 6L, arrowheads).

The expression of *Fgf8* relative to the areas of cell death seen in *Fgf8*$^{neo/-}$ embryos coupled with the phenotype later seen in these mutants strongly suggests that *Fgf8* is required for migrating NCC survival. To indirectly examine whether some of the cells dying are in fact neural crest, we first compared whole-mount lineage-traced neural crest expression to the areas of cell death. NCCs were marked by *lacZ* using the *P0-Cre* transgenic line crossed to the Cre reporter *R26R* (Fig. 6O). When compared with the pattern of cell death in the lateral optical section of a stage-matched *Fgf8* mutant (Fig. 6N), the pattern of expression strikingly matches that of the NCCs, suggesting that some of the pharyngeal arch NCCs are dying in *Fgf8* mutants (compare Figs 5A-D, 6O with 6N).

To determine definitively that some NCCs are dying in *Fgf8* mutants, we examined lineage-traced NCCs in *Fgf8* mutants for cell death. Using TUNEL assay on *R26R*::*P0-Cre*::

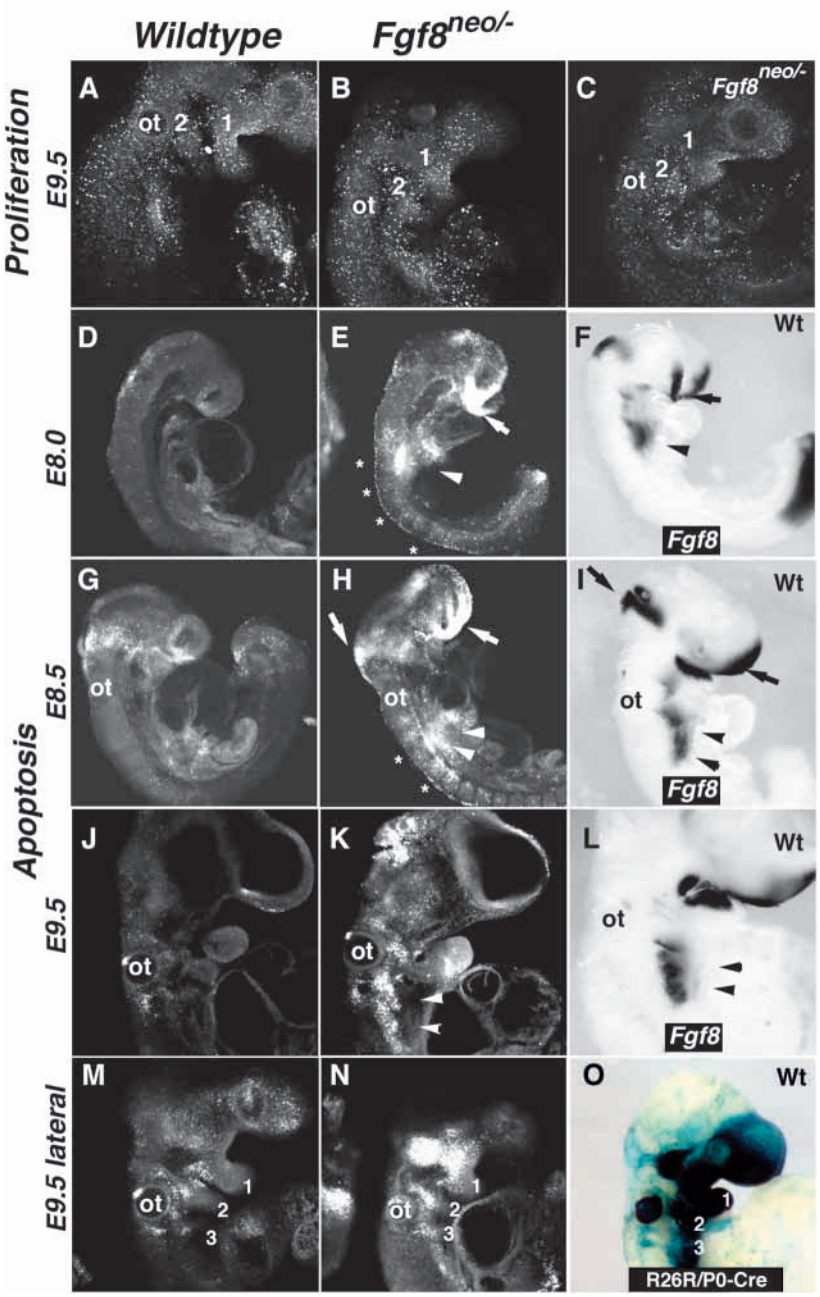

Fig. 6. Proliferation within the developing arches appeared grossly the same between wild type (A) and *Fgf8* mutants (B,C). Examination of cell death between E8.0-E9.5 revealed a striking pattern of increased cell death in *Fgf8* mutants. In E8.0-8.5 *Fgf8* mutants (E), there was increased death along the flank near the cardiac inflow (arrowheads, E,H) as well as along the dorsal axis (stars, E,H) and anterior neural ridge (E, arrow) when compared with control embryos (D,G). At E9.5, there was increased cell death within the caudal arches (arrowheads, K) and cells entering the arches (N) of *Fgf8* mutants when compared with controls (J,M). At E9.5 the pattern of cell death was similar to that of lineage traced NCCs in wild-type embryos using *P0-Cre* and the Cre reporter *R26R*. (compare M, N with O). Strikingly, the mRNA expression of *Fgf8* in wild-type embryos closely matched the areas of cell death (compare F,I,L with E,H,K, respectively). ot, otocyst.

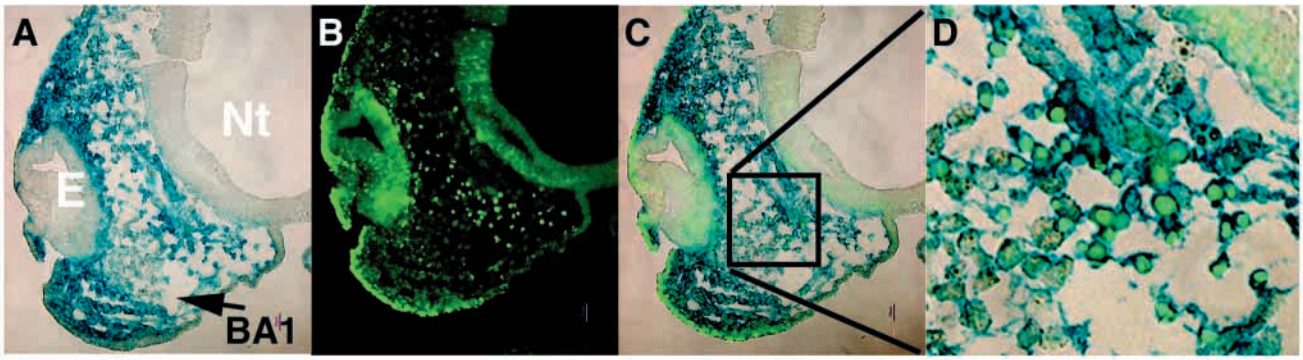

Fig. 7. TUNEL analysis in E10.5 *PO-Cre*::*R26R*::*Fgf8*$^{Neo/-}$ mutant demonstrates NCCs that are dying. Frontal section through first PA demonstrates β-Gal-positive cells (A), TUNEL-positive cells (B) and overlap (C). Blow up of boxed area in C clearly demonstrates double labeled (*lacZ* and TUNEL positive) cells (D). Nt, neural tube; E, eye; BA1, pharyngeal arch 1.

Fgf8$^{neo/-}$ embryos, we detected mesenchymal cells that were blue (Fig. 7A), apoptotic (Fig. 7B) and overlapping (Fig. 7C). Closer examination of the overlap (Fig. 7D) revealed the expected nuclear localization of the TUNEL product as well as the cytoplasmic β-gal activity.

It should be noted that while the cell death seen in some areas of *Fgf8* mutants occur in areas of NCC migration (Fig. 6N), many of the cells that are dying are clearly not NCCs based on location and stage of development. For example, the area of cell death near the cardiac inflow area at E8.0 (Fig. 6E) is present prior to any NCCs entering this area, indicating that *Fgf8* is required for survival of other cell types besides the NCCs.

Fgf8$^{neo/-}$ embryos resemble *Tbx1*$^{-/-}$ embryos

Recently, the T-box containing transcription factor *Tbx1*, which is present in the human 22q11 deletion region, has been shown to be required for pharyngeal arch and cardiovascular development when deficient in the mouse. *Tbx1*$^{-/-}$ embryos have multiple defects in heart development as well defects in the tympanic ring, zygomatic arch, temporal bone, external ear, palate and thymus (Jerome and Papaioannou, 2001). In addition, the pharyngeal arches are markedly hypoplastic (Vitelli et al., 2002a). All of these defects are observed in *Fgf8* mutants (Fig. 4). Therefore we next sought to determine if *Fgf8* and *Tbx1* are in a common molecular pathway of arch/NCC development.

Fgf8 is not required for *Tbx1* expression

To determine if expression of *Tbx1* requires *Fgf8*, we examined the expression of *Tbx1* mRNA in *Fgf8*$^{neo/-}$ embryos at E9.5 and E10.5. While the embryos examined had hypoplastic arches, *Tbx1* was clearly expressed in these mutants (n=8), suggesting *Fgf8* is not required to induce *Tbx1* (Fig. 8A,B). However there

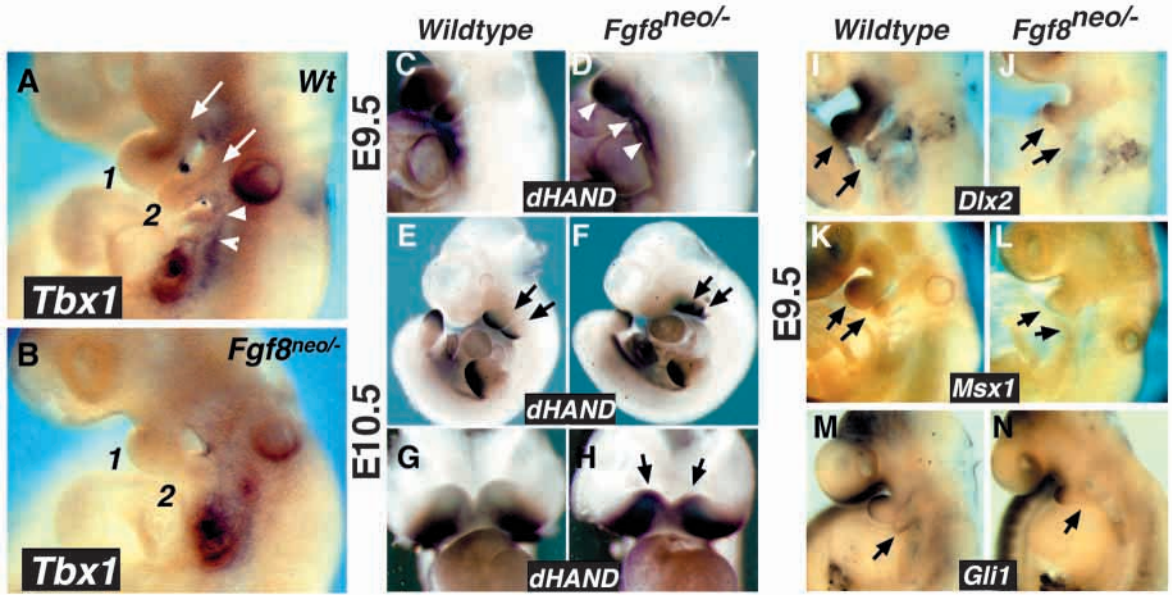

Fig. 8. mRNA in situ hybridization at E9.5 demonstrates loss of *Tbx1* expression in the core of the first and second arch in mutant (B) when compared with control (arrows A). In addition there was no expression in the area of the third arch artery (arrowheads, compare A with B). Expression of *dHAND* was maintained or expanded in *Fgf8* mutants (D,F) compared with wild type (C,E). Frontal view of first arch reveals possible expansion of *dHAND* in *Fgf8* mutants (G,H). Expression of *Dlx2*, (I,J) *Msx1* (K,L) and *Gli1* (M,N) were reduced or absent in the arches (arrows), particularly in PA2 with very distal sparing in PA1.

was loss of *Tbx1* expression in the core of the first and second arches as well as around the developing third arch artery (6/8). This most probably indicates that the tissues that normally express *Tbx1* were absent; however, we cannot rule out that *Fgf8* may be required to maintain, but not induce, some domains of *Tbx1* expression such as in the core of PA1 and PA2 (Fig. 8).

As *Fgf8*$^{neo/-}$ embryos have reduced but not completely absent *Fgf8* transcript levels, it is also theoretically possible that *Tbx1* induction does require *Fgf8*, but the low level of *Fgf8* message present is adequate to induce, but not to maintain, *Tbx1*. In order to test whether *Fgf8* can induce *Tbx1*, we applied beads coated with FGF8 protein to the arches of E9.5 and E10.5 wild-type embryos (see Materials and Methods) and (Garg et al., 2001). We were unable to detect any change in the normal expression of *Tbx1* by FGF8 despite the ability of the beads to induce Gbx2 in neural tissue (data not shown). These data strongly suggest that if *Fgf8* and *Tbx1* share a common genetic pathway, *Fgf8* is downstream of *Tbx1*.

dHAND expression is maintained in *Fgf8*$^{neo/-}$ hypoplastic arches

One other potentially important arch developmental gene that may be regulated by *Fgf8* is the basic helix loop helix transcription factor *dHAND* (*Hand2* – Mouse Genome Informatics). *dHAND* is expressed in the pharyngeal arches and has been implicated in NCC development as *dHAND*$^{-/-}$ embryos have hypoplasia of the pharyngeal arches as well as cardiovascular patterning defects (Thomas et al., 1998). The arch defects seen in *dHAND* null embryos are reminiscent of the hypoplasia seen in *Fgf8* mutants. In addition, *dHAND* expression requires endothelin 1 (*Et1*) signaling (Charite et al., 2001; Clouthier et al., 2000), and *Fgf8* is required for *Et1* expression in the first PA (Trumpp et al., 1999). We therefore examined the expression of *dHAND* in *Fgf8* mutant embryos. Surprisingly, *dHAND* expression was conserved or even expanded in *Fgf8* mutants, despite the presence of severely hypoplastic arches at E9.5 (Fig. 8C,D and data not shown). At E10.5, expression continued to be maintained despite almost complete absence of arches 1 and 2 (Fig. 8E,F, arrows). Examination of the medial first arch in these same embryos revealed an apparent expansion of the *dHAND* domain in the *Fgf8* mutant (Fig. 8G,H). One possible explanation for this finding is that the distal tips of the pharyngeal arches are maintained while the more proximal domains are lost, which is consistent with previous findings in the first arch (Trumpp et al., 1999; Tucker et al., 1999). To test this we examined three more markers expressed in the arches at E9.5. *Dlx2* is a member of the distal-less gene family and is expressed in the mesenchyme of arches 1 and 2 (Qiu et al., 1995). *Fgf8* mutants consistently had reduced expression of *Dlx2* in the first arch and absent expression in arch 2 (Fig. 8I,J). Similarly, the homeobox gene *Msx1*, which is thought to be regulated by *dHAND* (Thomas et al., 1998), was reduced or absent in arch 1 and 2, while present in the distal tip of wild type (Fig. 8K,L). Finally, the transcription factor *Gli1*, a target of the hedgehog signaling pathway, is also expressed in the developing arches (Platt et al., 1997). *Shh*$^{-/-}$ mutants also have hypoplastic (Chiang et al., 1996) arches with increased cell death (E. N. M., unpublished). *Gli1* expression was retained in the distal PA1 but was absent from PA2 in *Fgf8* mutants (Fig. 8M,N) consistent with the *dHAND* and *Dlx2* findings. All of these data suggest that distal first PA signaling is relatively spared, while second PA derivatives are absent in *Fgf8* mutants. We suggest that these pathways are primarily affected by the loss of tissue and not through direct regulation by *Fgf8*, except possibly that *dHAND* expression may be restricted by *Fgf8*.

DISCUSSION

We have demonstrated that *Fgf8* mutants have defects in cardiovascular patterning, including hypoplastic arch arteries and deficient outflow tract septation, primarily resulting in transposition with double outlet right ventricle and less frequently persistent truncus arteriosus. Other cardiac defects include atrial and ventricular septal defects, as well as atrioventricular valve defects. In addition, there are defects in craniofacial development involving the palate, mandible, middle ear bones, thyroid and external ear that, all together, suggest defects in NCC development caused by decreased *Fgf8* function**.**

The constellation of craniofacial and cardiovascular abnormalities seen in the *Fgf8* mutant are reminiscent of defects seen in mouse embryos that disrupt the syntenic region of human chromosome 22q and are thought to result from defective NCC development. Recent evidence suggests that the T-Box transcription factor *Tbx1* is a critical gene within this chromosomal deletion (Jerome and Papaioannou, 2001; Lindsay et al., 2001; Merscher et al., 2001). Although there is strong evidence that *Tbx1* is a critical gene within the 22q11 critical region in the mouse, humans with a del22q11-like phenotype but not the deletion have yet to be found with a defect in the *Tbx1* gene (Gong et al., 2001). Inheritance patterns and other data strongly suggest the presence of modifying factors that may alter the phenotype of the del22q11 syndrome (Taddei et al., 2001). Because of the similarities in phenotype, it is tempting to speculate that *Fgf8* may be a *Tbx1* modifying factor. This is a reasonable hypothesis as there is evidence for *Fgf* regulation by T-box genes in other areas of development (Griffin et al., 1998; Rodriguez-Esteban et al., 1999), as well as a requirement of Fgfs for T-box gene function (Casey et al., 1998; Strong et al., 2000). More specifically, Tbx6 is not expressed in *Fgf8*$^{-/-}$ embryos (Sun et al., 1999).

We have demonstrated that *Tbx1* is expressed in *Fgf8* mutants but that the expression is reduced in the core of rostral arches, as well as around the third arch artery. This loss of expression appeared to correlate with lost tissue and most probably does not represent a direct effect on *Tbx1* expression. FGF2 has been shown to induce *Tbx4* and *Tbx5* rapidly in the chick (Isaac et al., 2000). However, when we placed FGF8 protein on E9.5 mouse PAs, we could not induce *Tbx1*, suggesting that *Fgf8* is not capable of inducing *Tbx1*. One caveat to this experiment is that we may have attempted to induce *Tbx1* at a time when the tissue was no longer competent to respond to *Fgf8*. However, it is more likely that *Fgf8* cannot regulate *Tbx1*. These data suggest that if *Fgf8* shares a common signaling pathway with *Tbx1*, *Fgf8* lies downstream of *Tbx1*. Data from Vitelli et al. (Vitelli et al., 2002b) support this model as *Fgf8* is not expressed in the endoderm of *Tbx1*$^{-/-}$ embryos and *Fgf8*$^{+/-}$::*Tbx1*$^{+/-}$ double heterozygous embryos have an enhanced phenotype over that of *Fgf8*$^{+/+}$::*Tbx1*$^{+/-}$ embryos.

While there is evidence of some interaction, there are several differences in the phenotypes of *Fgf8*$^{neo/-}$ embryos and *Tbx1*$^{-/-}$ embryos. Disruption of NCC migration is seen in *Tbx1*$^{-/-}$ embryos (Vitelli et al., 2002a) but not in *Fgf8* mutants (Fig. 5B,D) suggesting different mechanisms of action. *Tbx1*$^{+/-}$ embryos are also haplo-insufficient and have a low frequency of defects in aortic arch artery development. We examined 23 *Fgf8*$^{+/-}$ embryos at E10.5 for defects in arch artery development and found only one with abnormal arch artery patterning when compared with wild-type controls. In addition, we found that 196/418 (47% of predicted 50%) *Fgf8*$^{+/-}$ mice were present at weaning age, suggesting no significant increased perinatal or neonatal lethality in heterozygous embryos. *Tbx1*$^{-/-}$ embryos also are reported to have defects in first and second cervical vertebrae and fusion of the basisphenoid/basiocciptal bones (Jerome and Papaioannou, 2001). We did not observe these defects in *Fgf8* mutants.

One other genetic pathway we have investigated is that of the HAND transcription factors. *dHAND* is reported to be a downstream target of the endothelin pathway gene *Et1* (Clouthier et al., 2000). *Et1*$^{-/-}$ embryos and knockouts of the endothelin receptors have cardiovascular and other defects that resemble the defects we observed in *Fgf8* mutants and *Et1* is reported to require *Fgf8* for expression. Although most genes examined (*Dlx2*, *Msx1* and *Gli1*) were reduced or absent from the arches of *Fgf8* mutants, *dHAND* was normal or expanded, suggesting a possible complex regulatory loop between the *dHAND* gene and *Fgf8* that we are investigating further.

Cardiovascular defects due to L-R axis and NCC abnormalities

How reduction of *Fgf8* results in the cardiovascular defects described remains unclear. It seems likely that the arch artery defects are due to hypoplasia of the pharyngeal arches and/or loss of NCCs. It also seems likely that the intracardiac defects may be related to LR defects and not necessarily NCC development. However, how transposition and double outlet right ventricle occur is less clear. *Fgf8* mutants clearly have defects in several neural crest-derived structures and have a moderate amount of NCC death. Our NCC lineage trace indicates that fewer NCCs are entering the outflow tract of the heart, and, in the case of one mutant, little or no NCCs were seen entering the outflow tract. It is tempting to speculate that decreased NCCs entering the outflow tract results in defects such as double outlet right ventricle, and that more severe reductions of NCCs result in persistent truncus arteriosus. This is consistent with the findings of M. Kirby and colleagues who demonstrated that ablation of neural crest can lead to double outlet right ventricle rather than persistent truncus arteriosus, possibly owing to ‘partial’ NCC ablation (Kirby and Waldo, 1995). It is also consistent with the observation that individuals with del22q11 have a range of cardiac defects that include outflow tract defects other than persistent truncus arteriosus.

However, these cardiac defects must also be considered with the knowledge that ~50% of *Fgf8* mutants are predicted to have defects in LR axis in the form of right isomerism, while 30% have cardiac looping reversals. Reversal of looping results in atrioventricular discordance (right atria with left ventricle, left atria with right ventricle). This does not necessarily result in outflow tract defects, as the alignment of ventricles with the outflow tract arteries may be independent of the alignment with the atria. However, some evidence suggests that abnormal LR axis specification does result in outflow tract defects, as other mouse models of right isomerism also frequently demonstrate outflow tract defects such as double outlet right ventricle (reviewed by Kathiriya and Srivastava, 2000). Whether there are also pharyngeal arch and/or NCC abnormalities in these genetic models remains to be determined.

It seems clear that all of the cardiovascular defects could result from either alterations in LR axis specification or NCCs or some combination of both. In fact, it is hypothetically possible that LR signals pattern NCCs as these streams enter the arches and the outflow tract as distinct left and right populations (E. N. M., unpublished). LR differences in NCCs could theoretically account for why arch arteries regress/remain asymmetrically with respect to left and right.

In addition to neural crest and LR axis problems, *Fgf8* mutants also have defects in endoderm formation (Fig. 3). There is a apparent loss of endoderm structures, and the caudal pharyngeal pouches do not express *Pax1* in *Fgf8*$^{neo/-}$ embryos. Pharyngeal endoderm has previously been proposed as crucial for NCC development (Couly et al., 2002). Recent evidence suggests that cells are added from the pharyngeal tissue and contribute to the lengthening of the outflow tract (Kelly et al., 2001; Mjaatvedt et al., 2001; Waldo et al., 2001). Loss of these cells could also theoretically result in shortening of the outflow tract and subsequently malalignment, such as double outlet right ventricle. Tissue-specific Cre transgenics that are expressed in the endoderm exclusive of the ectoderm, or vice versa, could be used to address which or if both expression domains are important for what defects by eliminating complicating LR patterning defects.

How does *Fgf8* affect NCCs

FGFs have been shown to influence proliferation, differentiation, migration, and survival of cells depending on the developmental context (reviewed by Ornitz and Itoh, 2001). *Fgf8* is expressed in several domains that could affect NCC development (Crossley and Martin, 1995) and has previously been proposed to be important for pharyngeal arch development based on its expression pattern (Wall and Hogan, 1995). Between E7.5 and E8.0, *Fgf8* is expressed in the primitive streak and the developing tail as the embryonic axis extends (Fig. 6F). Theoretically, *Fgf8* in these domains could be important for the specification of NCC precursors that will form at the border between neural and non-neural ectoderm, as has previously been suggested for Fgfs in vitro (Villanueva et al., 2002) (reviewed by Baker and Bronner-Fraser, 1997).

Fgf8 has also been implicated in NCC migration and specification (Kubota and Ito, 2000; Trainor et al., 2002). However, most or all of the NCCs appear to be specified and to migrate properly in *Fgf8* mutants, so that the primary defects appear to result from the partial failure of NCC survival as they migrate and enter the pharyngeal arches. *Fgf8* is expressed in the overlying arch ectoderm as well as the pharyngeal endoderm, which are in approximation with the migrating NCCs in all of the developing arches. Either or both of these domains of expression may therefore be crucial to maintain NCCs directly or indirectly. The importance of *Fgf8* expression within first arch ectoderm for NCC survival has previously been demonstrated (Trumpp et al., 1999; Tucker et al., 1999). The expression of *Fgf8* in the arches is dynamic, with more

diffuse expression early as each arch forms (Fig. 6F,I), and more restricted expression as the arch becomes more defined (Fig. 6L). Our data suggest that similar to the first PA, *Fgf8* expression in lower arches (ectodermal and/or endodermal) is required for NCC survival.

In summary, we have demonstrated that *Fgf8* mutants have NCC defects that resemble some aspects of the 22q11 deletion syndromes. NCCs are specified and migrate in *Fgf8* mutants, but undergo cell death in the absence of normal *Fgf8* mRNA levels. Although *Fgf8* mutants resemble *Tbx1*$^{-/-}$ mouse embryos, whether *Tbx1* acts on NCCs through *Fgf8* remains to be determined. Cardiac and craniofacial defects in these mutants most likely result from loss of NCCs in combination with abnormal specification of the LR axis. Whether *Fgf8* affects NCCs directly or indirectly and what domains of *Fgf8* expression are crucial for NCC survival are areas we are investigating further. A variety of genetic and in vitro manipulations should help to answer these questions.

We are very grateful to P. Soriano and T. Sato for providing *R26R* and *Tie2-lacZ* transgenic mice, respectively. We thank R. Anderson and M. Sullivan for technical assistance and M. Kirby, J. Klingensmith and members of his laboratory for critical reading of this manuscript. We thank D. Srivastava (Tbx1), P. Gruss (Pax1), R. Tijan (Ap2) and U. Erikson (CrabP1), A. Joyner (Gli1), J. Rubenstein (Dlx2) and R. Maxson (Msx1) for probes. Funded in part by NIH NICHD HD42803 and HD01216.

REFERENCES

Alsan, B. H. and Schultheiss, T. M. (2002). Regulation of avian cardiogenesis by Fgf8 signaling. *Development* **129**, 1935-1943.

Baker, C. V. and Bronner-Fraser, M. (1997). The origins of the neural crest. Part I: Embryonic induction. *Mech. Dev.* **69**, 3-11.

Casey, E. S., O'Reilly, M. A., Conlon, F. L. and Smith, J. C. (1998). The T-box transcription factor Brachyury regulates expression of eFGF through binding to a non-palindromic response element. *Development* **125**, 3887-3894.

Charite, J., McFadden, D. G., Merlo, G., Levi, G., Clouthier, D. E., Yanagisawa, M., Richardson, J. A. and Olson, E. N. (2001). Role of Dlx6 in regulation of an endothelin-1-dependent, dHAND branchial arch enhancer. *Genes Dev.* **15**, 3039-3049.

Chiang, C., Litingtung, Y., Lee, E., Young, K. E., Corden, J. L., Westphal, H. and Beachy, P. A. (1996). Cyclopia and defective axial patterning in mice lacking Sonic hedgehog gene function. *Nature* **383**, 407-413.

Clouthier, D. E., Williams, S. C., Yanagisawa, H., Wieduwilt, M., Richardson, J. A. and Yanagisawa, M. (2000). Signaling pathways crucial for craniofacial development revealed by endothelin-A receptor-deficient mice. *Dev. Biol.* **217**, 10-24.

Couly, G., Creuzet, S., Bennaceur, S., Vincent, C. and le Douarin, N. M. (2002). Interactions between Hox-negative cephalic neural crest cells and the foregut endoderm in patterning the facial skeleton in the vertebrate head. *Development* **129**, 1061-1073.

Crossley, P. H. and Martin, G. R. (1995). The mouse Fgf8 gene encodes a family of polypeptides and is expressed in regions that direct outgrowth and patterning in the developing embryo. *Development* **121**, 439-451.

Dencker, L., Annerwall, E., Busch, C. and Eriksson, U. (1990). Localization of specific retinoid-binding sites and expression of cellular retinoic-acid-binding protein (CRABP) in the early mouse embryo. *Development* **110**, 343-352.

Deutsch, U., Dressler, G. R. and Gruss, P. (1988). Pax 1, a member of a paired box homologous murine gene family, is expressed in segmented structures during development. *Cell* **53**, 617-625.

Farrell, M. J., Burch, J. L., Wallis, K., Rowley, L., Kumiski, D., Stadt, H., Godt, R. E., Creazzo, T. L. and Kirby, M. L. (2001). FGF-8 in the ventral pharynx alters development of myocardial calcium transients after neural crest ablation. *J. Clin. Invest.* **107**, 1509-1517.

Garg, V., Yamagishi, C., Hu, T., Kathiriya, I. S., Yamagishi, H. and Srivastava, D. (2001). Tbx1, a DiGeorge syndrome candidate gene, is regulated by sonic hedgehog during pharyngeal arch development. *Dev. Biol.* **235**, 62-73.

Gong, W., Gottlieb, S., Collins, J., Blescia, A., Dietz, H., Goldmuntz, E., McDonald-McGinn, D. M., Zackai, E. H., Emanuel, B. S., Driscoll, D. A. et al. (2001). Mutation analysis of TBX1 in non-deleted patients with features of DGS/VCFS or isolated cardiovascular defects. *J. Med. Genet.* **38**, E45.

Griffin, K. J., Amacher, S. L., Kimmel, C. B. and Kimelman, D. (1998). Molecular identification of spadetail: regulation of zebrafish trunk and tail mesoderm formation by T-box genes. *Development* **125**, 3379-3388.

Isaac, A., Cohn, M. J., Ashby, P., Ataliotis, P., Spicer, D. B., Cooke, J. and Tickle, C. (2000). FGF and genes encoding transcription factors in early limb specification. *Mech. Dev.* **93**, 41-48.

Jerome, L. A. and Papaioannou, V. E. (2001). DiGeorge syndrome phenotype in mice mutant for the T-box gene, Tbx1. *Nat. Genet.* **27**, 286-291.

Jiang, X., Rowitch, D., Soriano, P., McMahon, A. P. and Sucov, H. (2000). Fate of the mammalian cardiac neural crest. *Development* **127**, 1607-1616.

Kathiriya, I. S. and Srivastava, D. (2000). Left-right asymmetry and cardiac looping: implications for cardiac development and congenital heart disease. *Am. J. Med. Genet.* **97**, 271-279.

Kelly, R. G., Brown, N. A. and Buckingham, M. E. (2001). The arterial pole of the mouse heart forms from Fgf10-expressing cells in pharyngeal mesoderm. *Dev. Cell* **1**, 435-440.

Kirby, M. L. and Waldo, K. L. (1995). Neural crest and cardiovascular patterning. *Circ. Res.* **77**, 211-215.

Kubota, Y. and Ito, K. (2000). Chemotactic migration of mesencephalic neural crest cells in the mouse. *Dev. Dyn.* **217**, 170-179.

Kuratani, S. C. and Kirby, M. L. (1992). Migration and distribution of circumpharyngeal crest cells in the chick embryo. Formation of the circumpharyngeal ridge and E/C8+ crest cells in the vertebrate head region. *Anat. Rec.* **234**, 263-280.

Lewandoski, M., Sun, X. and Martin, G. (2000). Fgf8 signalling from the AER is essential for normal limb development. *Nat. Genet.* **26**, 460-463.

Li, J., Chen, F. and Epstein, J. A. (2000). Neural crest expression of Cre recombinase directed by the proximal Pax3 promoter in transgenic mice. *Genesis* **26**, 162-164.

Lindsay, E. A. (2001). Chromosomal microdeletions: dissecting del22q11 syndrome. *Nat. Rev. Genet.* **2**, 858-868.

Lindsay, E. A. and Baldini, A. (2001). Recovery from arterial growth delay reduces penetrance of cardiovascular defects in mice deleted for the DiGeorge syndrome region. *Hum. Mol. Genet.* **10**, 997-1002.

Lindsay, E. A., Vitelli, F., Su, H., Morishima, M., Huynh, T., Pramparo, T., Jurecic, V., Ogunrinu, G., Sutherland, H. F., Scambler, P. J. et al. (2001). Tbx1 haploinsufficieny in the DiGeorge syndrome region causes aortic arch defects in mice. *Nature* **410**, 97-101.

Maschhoff, K. L. and Baldwin, H. S. (2000). Molecular determinants of neural crest migration. *Am. J. Med. Genet.* **97**, 280-288.

Merscher, S., Funke, B., Epstein, J. A., Heyer, J., Puech, A., Lu, M. M., Xavier, R. J., Demay, M. B., Russell, R. G., Factor, S. et al. (2001). TBX1 is responsible for cardiovascular defects in velo-cardio- facial/DiGeorge syndrome. *Cell* **104**, 619-629.

Meyers, E. N. and Martin, G. R. (1999). Differences in left-right axis pathways in mouse and chick: functions of FGF8 and SHH. *Science* **285**, 403-406.

Meyers, E. N., Lewandoski, M. and Martin, G. R. (1998). An Fgf8 mutant allelic series generated by Cre-and Flp-mediated recombination. *Nat. Genet.* **18**, 136-141.

Mitchell, P., Timmons, P., Herbert, J., Rigby, P. and Tijan, R. (1991). Transcription factor Ap-2 is exspressed in neural crest cell lineages during mouse embryogenesis. *Genes Dev.* **5**, 105-119.

Mjaatvedt, C. H., Nakaoka, T., Moreno-Rodriguez, R., Norris, R. A., Kern, M. J., Eisenberg, C. A., Turner, D. and Markwald, R. R. (2001). The outflow tract of the heart is recruited from a novel heart-forming field. *Dev. Biol.* **238**, 97-109.

Moon, A. M. and Capecchi, M. R. (2000). Fgf8 is required for outgrowth and patterning of the limbs. *Nat. Genet.* **26**, 455-459.

Neubuser, A., Peters, H., Balling, R. and Martin, G. R. (1997). Antagonistic interactions between FGF and BMP signaling pathways: a mechanism for positioning the sites of tooth formation. *Cell* **90**, 247-255.

Nishibatake, M., Kirby, M. L. and van Mierop, L. H. (1987). Pathogenesis of persistent truncus arteriosus and dextroposed aorta in the chick embryo after neural crest ablation. *Circulation* **75**, 255-264.

Ornitz, D. M. and Itoh, N. (2001). Fibroblast growth factors. *Genome Biol.* **2**, 3005.1-3005.12.

Platt, K. A., Michaud, J. and Joyner, A. L. (1997). Expression of the mouse Gli and Ptc genes is adjacent to embryonic sources of hedgehog signals suggesting a conservation of pathways between flies and mice. *Mech. Dev.* **62**, 121-135.

Qiu, M., Bulfone, A., Martinez, S., Meneses, J. J., Shimamura, K., Pedersen, R. A. and Rubenstein, J. L. (1995). Null mutation of Dlx-2 results in abnormal morphogenesis of proximal first and second branchial arch derivatives and abnormal differentiation in the forebrain. *Genes Dev.* **9**, 2523-2538.

Reifers, F., Walsh, E., Leger, S., Stainier, D. and Brand, M. (2000). Induction and differentiation of the zebrafish heart requires fibroblast growth factor 8 (fgf8/acerebellar). *Development* **127**, 225-235.

Rodriguez-Esteban, C., Tsukui, T., Yonei, S., Magallon, J., Tamura, K. and Izpisua Belmonte, J. C. (1999). The T-box genes Tbx4 and Tbx5 regulate limb outgrowth and identity. *Nature* **398**, 814-818.

Schlaeger, T. M., Bartunkova, S., Lawitts, J. A., Teichmann, G., Risau, W., Deutsch, U. and Sato, T. N. (1997). Uniform vascular-endothelial-cell-specific gene expression in both embryonic and adult transgenic mice. *Proc Natl Acad Sci USA* **94**, 3058-3063.

Schneider, R. A., Hu, D., Rubenstein, J. L., Maden, M. and Helms, J. A. (2001). Local retinoid signaling coordinates forebrain and facial morphogenesis by maintaining FGF8 and SHH. *Development* **128**, 2755-2767.

Soriano, P. (1999). Generalized lacZ expression with the ROSA26 Cre reporter strain. *Nat. Genet.* **21**, 70-71.

Strong, C. F., Barnett, M. W., Hartman, D., Jones, E. A. and Stott, D. (2000). Xbra3 induces mesoderm and neural tissue in Xenopus laevis. *Dev. Biol.* **222**, 405-419.

Sun, X., Meyers, E. N., Lewandoski, M. and Martin, G. R. (1999). Targeted disruption of Fgf8 causes failure of cell migration in the gastrulating mouse embryo. *Genes Dev.* **13**, 1834-1846.

Swiatek, P. J. and Gridley, T. (1993). Perinatal lethality and defects in hindbrain development in mice homozygous for a targeted mutation of the zinc finger gene Krox20. *Genes Dev.* **7**, 2071-2084.

Taddei, I., Morishima, M., Huynh, T. and Lindsay, E. A. (2001). Genetic factors are major determinants of phenotypic variability in a mouse model of the DiGeorge/del22q11 syndromes. *Proc. Natl. Acad. Sci. USA* **98**, 11428-11431.

Thomas, T., Kurihara, H., Yamagishi, H., Kurihara, Y., Yazaki, Y., Olson, E. N. and Srivastava, D. (1998). A signaling cascade involving endothelin-1, dHAND and msx1 regulates development of neural-crest-derived branchial arch mesenchyme. *Development* **125**, 3005-3014.

Trainor, P. A., Ariza-McNaughton, L. and Krumlauf, R. (2002). Role of the isthmus and FGFs in resolving the paradox of neural crest plasticity and prepatterning. *Science* **295**, 1288-1291.

Trumpp, A., Depew, M. J., Rubenstein, J. L., Bishop, J. M. and Martin, G. R. (1999). Cre-mediated gene inactivation demonstrates that FGF8 is required for cell survival and patterning of the first branchial arch. *Genes Dev.* **13**, 3136-3148.

Tucker, A. S., Yamada, G., Grigoriou, M., Pachnis, V. and Sharpe, P. T. (1999). Fgf-8 determines rostral-caudal polarity in the first branchial arch. *Development* **126**, 51-61.

Villanueva, S., Glavic, A., Ruiz, P. and Mayor, R. (2002). Posteriorization by FGF, Wnt and retinoic acid is required for neural crest induction. *Dev. Biol.* **241**, 289-301.

Vitelli, F., Morishima, M., Taddei, I., Lindsay, E. A. and Baldini, A. (2002a). Tbx1 mutation causes multiple cardiovascular defects and disrupts neural crest and cranial nerve migratory pathways. *Hum. Mol. Genet.* **11**, 915-922.

Vitelli, F., Taddei, I., Morishima, M., Meyers, E. N., Lindsay, E. A. and Baldini, A. (2002b). A genetic link between Tbx1 and fibroblast growth factor signaling. *Development* **129**, 4605-4611.

Waldo, K. L., Kumiski, D. and Kirby, M. L. (1996). Cardiac neural crest is essential for the persistence rather than the formation of an arch artery. *Dev. Dyn.* **205**, 281-292.

Waldo, K. L., Kumiski, D. H., Wallis, K. T., Stadt, H. A., Hutson, M. R., Platt, D. H. and Kirby, M. L. (2001). Conotruncal myocardium arises from a secondary heart field. *Development* **128**, 3179-3188.

Wall, N. A. and Hogan, B. L. (1995). Expression of bone morphogenetic protein-4 (BMP-4), bone morphogenetic protein-7 (BMP-7), fibroblast growth factor-8 (FGF-8) and sonic hedgehog (SHH) during branchial arch development in the chick. *Mech. Dev.* **53**, 383-392.

Yamauchi, Y., Abe, K., Mantani, A., Hitoshi, Y., Suzuki, M., Osuzu, F., Kuratani, S. and Yamamura, K. (1999). A novel transgenic technique that allows specific marking of the neural crest cell lineage in mice. *Dev. Biol.* **212**, 191-203.

Zucker, R. M., Hunter, E. S., 3rd and Rogers, J. M. (1999). Apoptosis and morphology in mouse embryos by confocal laser scanning microscopy. *Methods* **18**, 473-480.